Electronic Supplementary Material (ESI) for Green Chemistry

Supporting Information

The Effects of Polyolefin Structure and Source on Pyrolysis-Derived Plastic Oil Composition

Jiayang Wu[1], Zhen Jiang[1], Victor Sanfins Cecon[2], Greg Curtzwiler[2], Keith Vorst[2], Manos Mavrikakis[1], George W. Huber[1]*

[1] Department of Chemical and Biological Engineering, University of Wisconsin-Madison; Madison, WI 53706, USA

[2] Polymer and Food Protection Consortium, Department of Food Science and Human Nutrition, Iowa State University, Ames, IA 50011, USA

*Corresponding authors: gwhuber@wisc.edu

1. Materials:

Chemicals below were used as purchased.
C8-C40 paraffins calibration standard (Sigma Aldrich, Product No. 40147-U)
1-hexene (Sigma Aldrich, Product No. 240761, ≥99%)
cis-2-hexene (Sigma Aldrich, Product No. 538493, ≥99%)
1,5 hexene (Sigma Aldrich, Product No. 128554, ≥97%)
Hexane (Sigma Aldrich, Product No. 675393, ≥95%)
Toluene (Sigma Aldrich, anhydrous, Product No. 244511, 99.8%)
Dodecane (Sigma Aldrich, anhydrous, Product No. 297879, ≥99%)
Chloroform-d (CDCl3, Sigma Aldrich, Product No. 151823, ≥99.8 atom %D)
1,1,2,2-Tetrachloroethane-d_2 (Sigma Aldrich, Product No. 358703, ≥99.5 atom % D)
2-ethyl-1-butene (Sigma Aldrich, Product No. E14705, ≥95%)
1,4-hexadiene, mixture of cis and trans (Sigma Aldrich, Product No. 129186, ≥99%)
3,3-dimethyl-1-butene (Sigma Aldrich, Product No. 39832, ≥98.5%)
1-methylcyclopentene (Sigma Aldrich, Product No. M39806, ≥98%)
Methylcyclopentane (Sigma Aldrich, Product No. M39407, ≥97%)
Cyclohexene (Sigma Aldrich, Product No. 125431, ≥99%)
N,N-Dimethylformamide (Sigma Aldrich, Product No. 227056, ≥99.8%)
Heptane (Sigma Aldrich, Product No. 34873, ≥99%)
3,3-dimethyl-1-pentene (Sigma Aldrich, Product No. R289280)
2-ethyl-1-hexene (Sigma Aldrich, Product No. CDS000215)
2-methyl-1-hexene (Sigma Aldrich, Product No. 111627, ≥96%)
4-methyl-1-hexene (Sigma Aldrich, Product No. 67500, ≥98%)
2-methylhepatne (Sigma Aldrich, Product No. M47949, ≥98%)
1-octene (Sigma Aldrich, Product No. 74900, ≥99.5%)
1,7-octadiene (Sigma Aldrich, Product No. O2501, ≥98%)
1-nonene (Sigma Aldrich, Product No. 74323, ≥99.5%)
1-decene (Sigma Aldrich, Product No. 30650, ≥97%)
1,9-decadiene (Sigma Aldrich, Product No. 118303, ≥97%)
Decane (Sigma Aldrich, Product No. 457116, ≥99%)
1-undecene (Sigma Aldrich, Product No. 242527, ≥97%)
1-dodecene (Sigma Aldrich, Product No. 44148, ≥99%)
1-tetradecene (Sigma Aldrich, Product No. 87189, ≥97%)
1-pentadecene (Sigma Aldrich, Product No. 222887, ≥98%)
1-heptadecene (Sigma Aldrich, Product No. H1108, ≥98%)
Benzene (Sigma Aldrich, Product No. 12450, ≥99.9%)
P-xylene (Sigma Aldrich, Product No. 296333, ≥99%)
M-xylene (Sigma Aldrich, Product No. 296325, ≥99%)
O-xylene (Sigma Aldrich, Product No. 95662, ≥99%)
Ethylbenzene (Sigma Aldrich, Product No. 296848, ≥99.8%)
Styrene (Sigma Aldrich, Product No. S4972, >99%)
Propylbenzene (Sigma Aldrich, Product No. P52407, >98%)
Decahydronaphthalene (Sigma Aldrich, Product No. 8031010100, >99%)
Naphthalene (Sigma Aldrich, Product No. 147141, >99%)
1-methylnaphthalene (Sigma Aldrich, Product No. W319309, >95%)

2. Pyrolysis and distillation details

Pyrolysis of different plastics was carried out in a fluidized bed reactor. The scheme of the fluidized bed and product collection system is shown as Fig.S2. Residence time was calculated based on Equation S1.

$$\tau = \frac{volumetric\ flowrate\ of\ the\ N_2}{V_{reactor} - V_{sand}}$$ (Equation S1)

The volumetric gas flowrate was the gas flow rate at targeted temperature (500 ºC) and converted by the ideal gas law. The pyrolysis oil obtained from all condensers was mixed first in a round bottom flask and then distilled to a light cut and heavy cut to simplify the characterization. The distillation system is shown below. The round bottom flask was put in an oil bath with a stir bar and was heated up to 165 ºC by a hot plate and held isothermally for 10 minutes. The round bottom flask was also connected to a cylindrical condenser which was flowed through 10 ºC cold water to help condense the light oil. The light oil was collected by a round bottom flask which was connected to the cylindrical condenser through a bent adaptor and the round bottom flask was put in a dry ice container. A vacuum pump (Pfeiffer D-35614 Asslar) was connected to the adaptor. The actual boiling point of the oil cuts was around 175 ºC.

3. Plastic and Plastic Oils Characterizations

3.1 Attenuated Total Reflectance Fourier Transform Infrared Spectroscopy (ATR-FTIR)

ATR-FTIR was used to characterize the PCR plastics and the virgin resins. The instrument was a Bruker Vertex 70 with a liquid nitrogen cooled MCT detector. The ATR cell used was a MIRacle single reflection cell equipped with a diamond crystal (Pike Technologies). In a typical measurement, 128 scans were averaged with a 4 cm-1 resolution and range from 4000-400 cm^{-1}.

3.2 Gel Permeation Chromatography (GPC)

The molecular weight and molecular weight distribution of polyolefin samples were determined by dissolving specimens with a mass of 180-220 mg of polymer in HPLC grade 1,2,4-trichlorobenzene (TCB) (Fisher Scientific, Fair Lawn, NJ), containing 250 mg/L of 2,6-di-tert-butyl-4-methylphenol (BHT) (Sigma Aldrich, St. Louis, MO) as an antioxidant. This system was left under constant agitation and heated to 150°C for 5 hours for complete dissolution resulting in a concentration of 15 mg/mL. The samples were injected at a volume of 200 µL using a Malvern Viscotek 350 HT-GPC (Malvern Panalytical, Westborough, MA), equipped with an internal filtration system and refractive index (RI), viscometer, and light scattering (LS) detectors. Chromatographic separation occurred using a flow rate of 1.0 mL/min and an oven temperature of 145°C using two PLgel Olexis 300 x 7.5 mm columns (Agilent Technologies, Santa Clara, CA) in series with lower and higher molecular weight limits of 2,000 Da and 10,000,000 Da, respectively. A calibration curve was obtained using narrow polystyrene standards from 10,000 to 3,000,000 Da (Agilent Technologies, Santa Clara, CA) and converted for use with polyethylene using Mark-Houwink constants, as described in ASTM D6474-20 (ASTM, 2020b) with the WinGPC software (PSS USA, Amherst, MA).

3.3 Nuclear magnetic resonance (NMR)

Plastic: Each polymer (30 – 50mg) were added in 1 ml of 1,1,2,2-tetrachlorinethene-d2 and was heated in an oil bath (around 100 ºC) for 2 hours for dissolution. The dissolved polymers were then submitted to a Bruker Avance-500 NMR instrument with a BBFO probe and proceed the ^{13}C quantitative method at around 110 ºC (acquisition time: 1s, relaxation delay: 10s, number of scans: 10000, pulse sequence: zgig30). All the spectrums were processed through MestReNova.

Plastic oils: Each plastic oil (~0.5g) were added in 5ml $CDCl_3$ with 0.05g dimethylformamide (DMF) as internal standards. The samples were submitted to a Bruker Avance-500 NMR instrument with a DCH cryoprobe and proceed the normal ^{1}H method at room temperature (acquisition time: 3.27s, relaxation delay: 1s, number of scans: 32, pulse sequence: zg30). All the spectrums were processed through MestReNova.

3.4 GC analysis

GC×GC-FID

All oil samples were injected to the GC×GC. The GC×GC is equipped with a capillary Agilent 30 m VF-17ms column (CP8981) and a capillary Agilent 5 m DB-1 column (121-1011), flowed by hydrogen as the carrier gas with a flowrate at 2.5 ml/min. The inner diameter for both columns is 0.25mm. Series of chemicals were injected into GC×GC for the assignment of the blobs in the 2D chromatograph. The products were first injected into a column VF-17ms, which is mid-polarity and is used to separate compounds through polarity, then injected into DB-1 column, which does not have low polarity that can be used to separate compounds through the boiling points. For each measurement, the initial set temperature for the oven was 35 ºC and held for 4 min. The oven was then heated to 320 ºC with a ramping rate of 4 ºC/min and held at 320 ºC for another 15 min. Hydrogen was the carrier gas and the flow rate for hydrogen was 40 ml/min.

Heavy liquid GC

The linear hydrocarbons quantified through GC×GC system will be spliced into linear alkane, linear alkene, and linear alkadiene by the data obtained heavy liquid GC. The calibration signal is shown as Fig.S4B and Fig.S4C.

Heavy oil and whole oil sample was injected to the 1D GC for linear hydrocarbon analysis. The 1D GC is equipped with a Restek MXT-1HT column (Cat# 70132). The column length is 10 m with a 0.53 mm inner diameter. For each experiment, the initial set temperature for the oven was 35 ºC and held for 5 min. The oven was then heated to 415 ºC with a temperature ramping rate of 6 ºC/min and held at 415 ºC for another 6.15 min. Hydrogen was the carrier gas and the flow rate for hydrogen was 40 ml/min.

Refinery Gas Analyzer (RGA)

Gas products were analyzed using a Refinery Gas Analyzer GC-2014 (Shimadzu) with 1) Restek RTX–alumina column and an FID to analyze C1–C5 hydrocarbons and 2) RTX-Q-plot column and RTX-MS-5A column with a thermal conductivity detector (TCD) to quantify H2, respectively. The GC signal was calibrated with a commercial calibration mixture containing C1-C6 n-paraffins, C2-C6 olefins, and H2 standards (Scott Gas, 1000 ppm of each hydrocarbon and 10000 ppm H2).

3.5 Thermogravimetric Analysis (TGA)

TGA was carried out using a TA Instruments SDT Q500 system with nitrogen (N_2) used as the sweep gas. To study the polyolefin degradation, 10 mg PVC was heated to 320 °C with a temperature ramping rate of 2 °C/min and held at 320 °C isothermally for 20 min. To obtain the data for our kinetic model, 10 mg PVC was heated to 600 °C with a temperature ramping rate of 10 °C/min, and a flowrate of 200 sccm.

3.6 Inductively coupled plasma - optical emission spectrometry (ICP-OES)

Three replicates of 0.1500 ± 0.0005 g were collected for each sample and digested via microwave-assisted digestion using an UltraWave digestion system (Milestone, Inc., Shelton, CT) in 5 mL HNO3 67% v/v Trace Metal Grade (Fisher Scientific, Fair Lawn, NJ) and 1 mL HCl 34% v/v Trace Metal Grade (Fisher Scientific, Fair Lawn, NJ). Following instrument manufacturer instructions, an initial pressure of 40 bar with N_2 was applied, followed by a ramp of 10 min at a microwave power of 800 W from room temperature (22°C) to 110°C. Then another 10 min ramp was applied with 1200 W of power until 180°C, followed by a last 10 min ramp to 260°C with 1500 W of power. Then, the temperature and power settings were kept for 20 minutes until digestion ended.

The digested samples were diluted to 50 mL with ultra-pure, deionized water and assessed for metal content utilizing an ICP-OES (Thermo Scientific iCap-7400 Duo, Waltham, MA) instrument. The multi-element standards utilized for calibration contained 0.1 µg/L, 1 µg/L, 5 µg/L, 25 µg/L, 50 µg/L, and 100 µg/L of each metal tested, along with a 5 µg/L yttrium internal standard, all prepared from single

standard solutions of 1000 µg/L (Inorganic Ventures, Christiansburg, VA or Sigma-Aldrich, Saint Louis, MO). The analyzed samples were run with concurrent blanks (no polymer/oil) from each respective digestion batch with the goal to remove the effect of any potential contamination from metals present in the acids or leached from the digestion vessels.

3.7 Density functional theory (DFT) details

The thermochemistry and kinetics of all elementary steps of the chosen model compounds' pyrolysis were performed at the B3P86 level of theory with 6–31++g(d,p) basis set.[1, 2] Notably, we chose B3P86[3] rather than MP2[4] in our previous HDPE study[5] due to the small differences in the reaction Gibbs free energy and the activation energy barrier for C-C scission (below 5 kJ/mol, see Fig.S9, benchmarked in the C2H6 model) but much more reasonable computational cost. All the other six DFT functionals we examined, including WB97XD, M06-L, M06-2X, M05-2X, B3PW91, B3LYP, all with the same basis set delivered worse accuracy and higher computational cost than the selected B3P86. To determine transition states (TS) steps involving radicals, the free energy surface (FES) scan method with the minimum energy crossing point (MECP) at different electronic spin multiplicities was employed.[6-8] We added temperature corrections (T=500 ^{o}C) to the energetics for obtaining Gibbs free energies by vibrational frequency analysis on the structures obtained from the FES scan. The TS was confirmed by only one imaginary frequency corresponding to the reaction coordinate.

4. Feedstock and Reactor Schemes

4.1 The PCR plastic feedstocks

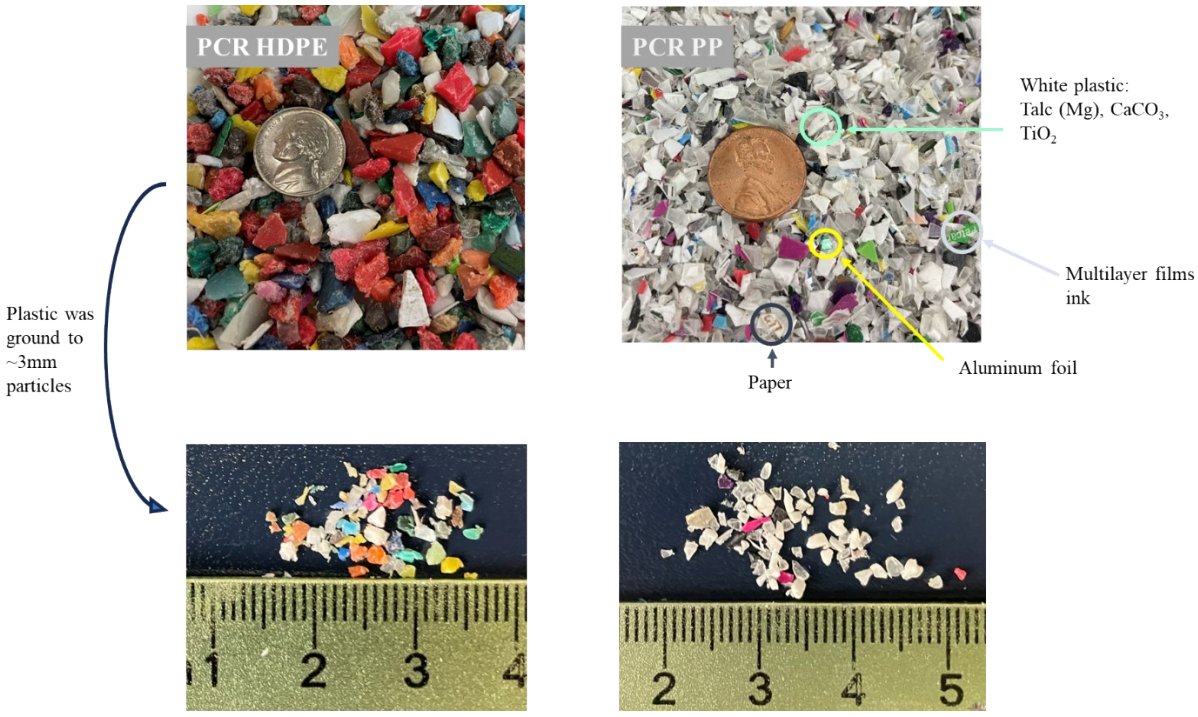

Fig.S1. Grinded PCR polyolefin feeds into the fluidized bed reactor

4.2 Scheme of the pyrolysis fluidized bed reactor

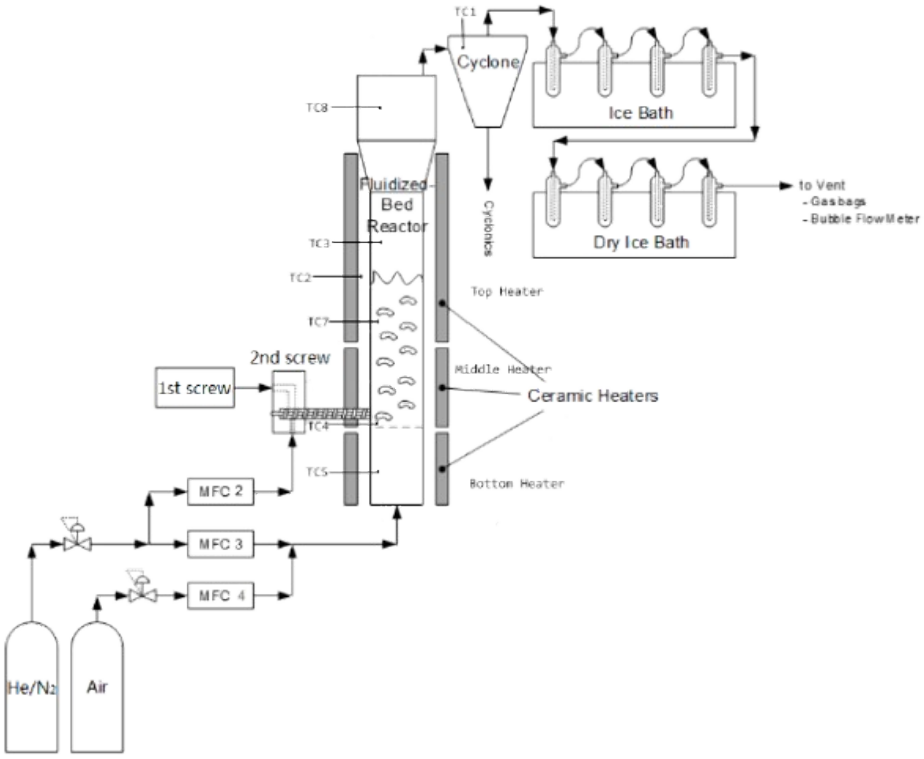

Fig.S2. The scheme of the fluidized bed reactor

5. Experimental and Computational Results

5.1 ATF-FTIR spectrum for PCR plastics

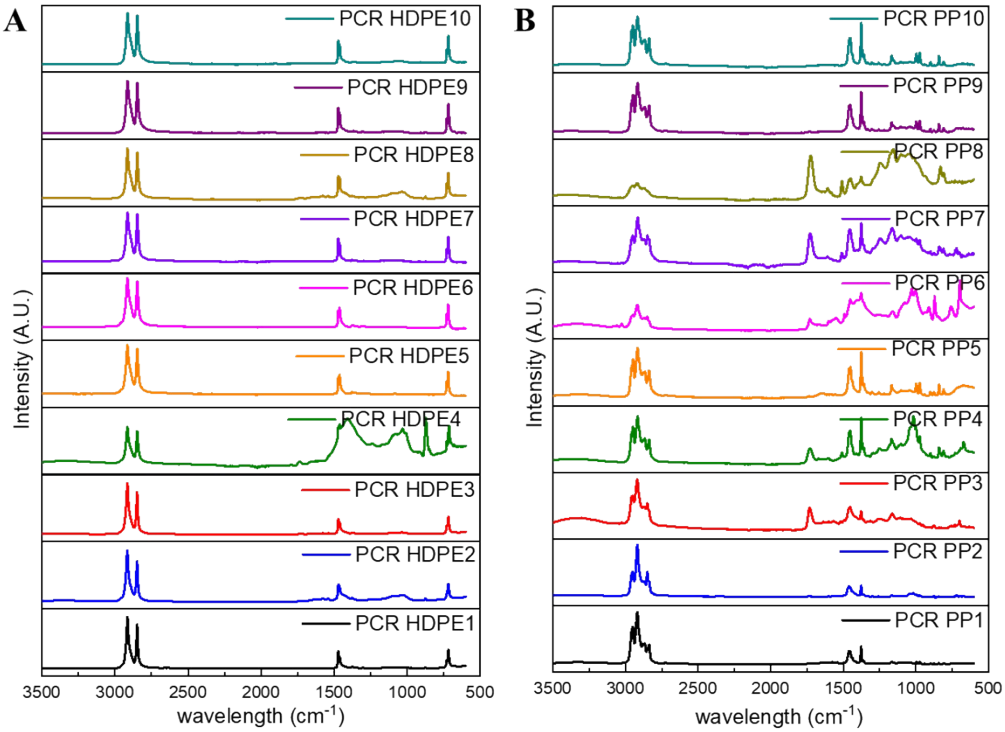

Fig.S3. All ten ATR-FTIR spectra for (A)PCR HDPE and (B)PCR PP

5.2 Detailed GC information

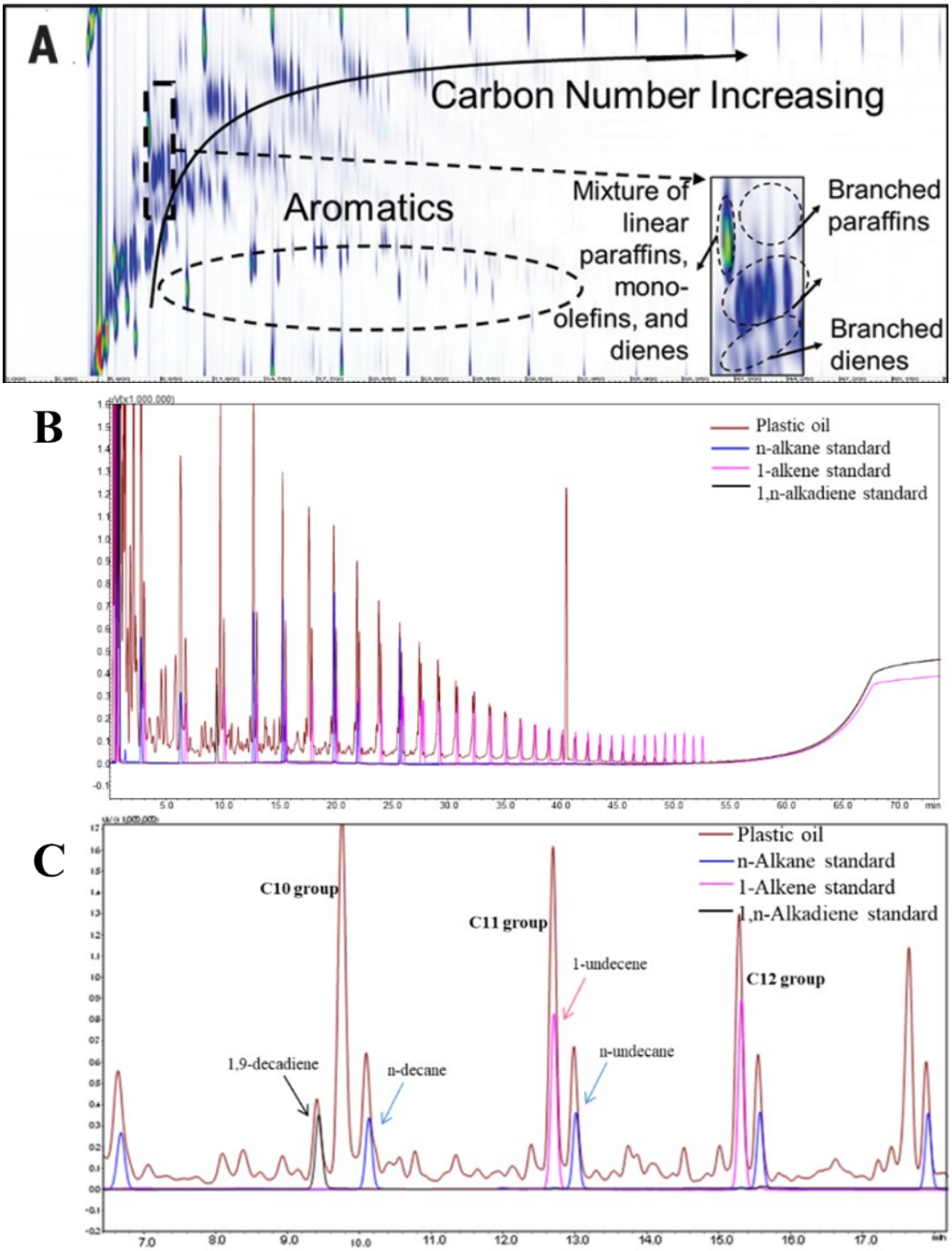

Fig.S4. (A) The template of GC×GC, (B)1D GC chromatograph of plastic pyrolysis oils and alkane, alkene, and alkadiene standards. (C) Zoomed in 1D GC results in the range of C10 to C12, showing the separation of linear alkane, alkene, and alkadiene.

5.3 Validation of 2D GC quantification results

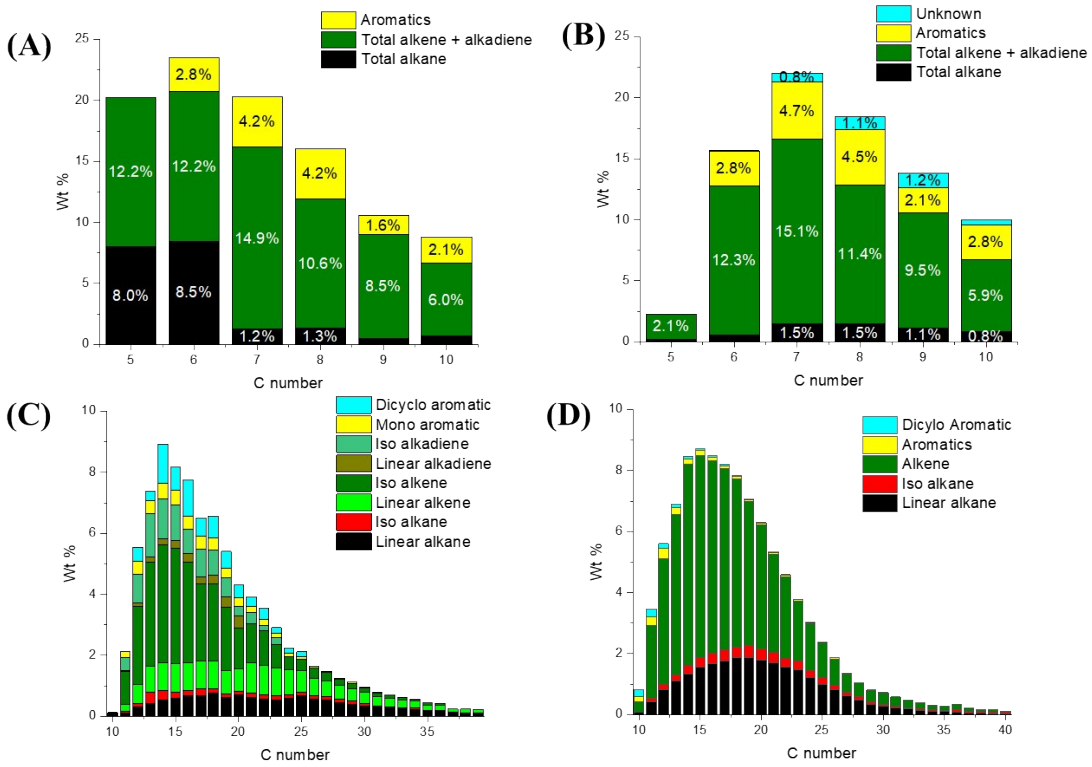

Fig.S5. Comparison of PCR HDPE distilled oils with GC×GC-FID results with NOISE and DHA (detailed hydrocarbon analysis) GC method. (A) GC×GC-FID results of light oil, (B) DHA results of light oil, (C) GC×GC-FID results of heavy oil, and (D) NOSIE analysis of heavy oil and the alkene includes liner alkene, iso alkene, linear alkadiene, and the iso alkadiene quantified through 2D GC.

5.4 Gas distribution quantified by RGA

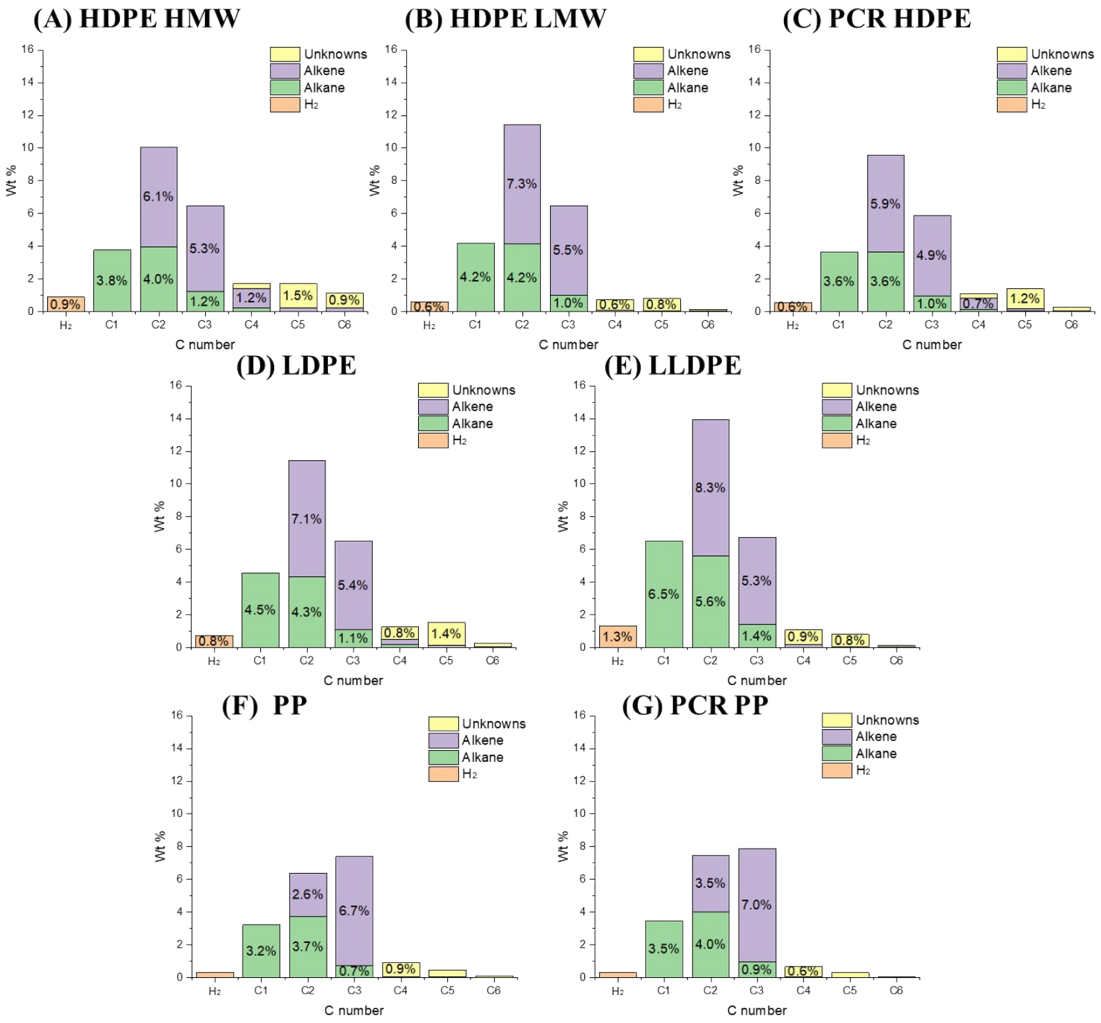

Fig. S6. The gas products of polyolefins pyrolysis quantified through refinery gas GC (RGA) of (A) HDPE HMW, (B) HDPE LMW, (C) PCR HDPE, (D) LDPE, (E) LLDPE, (F) PP, and (G) PCR PP

5.5 Zoomed in ^{1}H NMR spectrum of PCR HDPE and PP

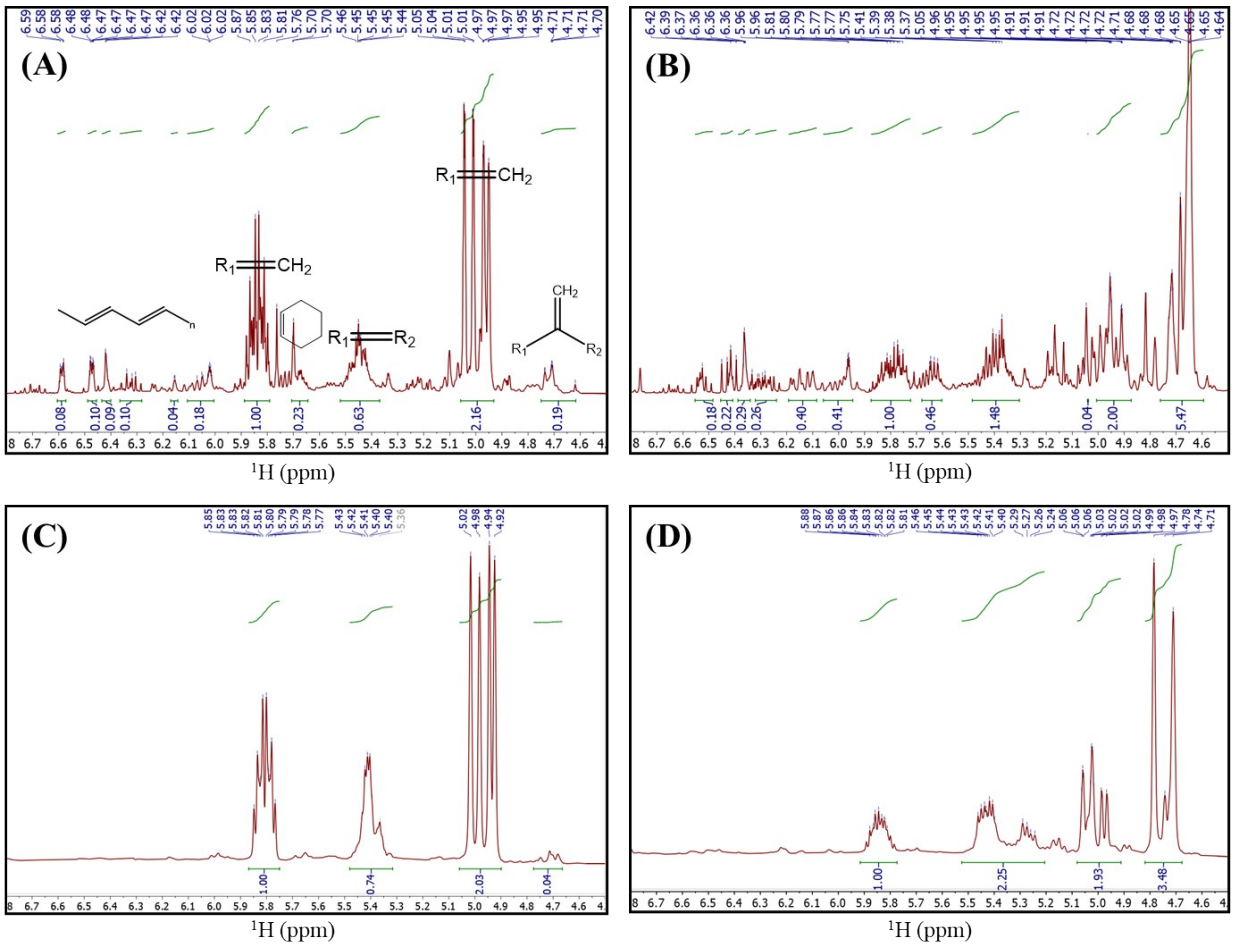

Fig. S7. ^{1}H NMR spectra of (A) PCR HDPE light oil, (B) PCR PP light oil, (C) PCR HDPE heavy oil, and (D) PCR PP heavy oil in $CDCl_3$ with dimethylformamide DMF as the internal standard.

According to the ^{1}H NMR, the oil contains 1,1- disubstituted olefins (4.7 ppm).[9, 10]

The chemical shift of the double bond in cyclohexene is from 5.6 ~5.7 ppm[11]

The chemical shift of conjugated dienes is from 6.2 ppm~ 6.7 ppm[10]

5.6 Branched compound distributions in seven types of plastic oils

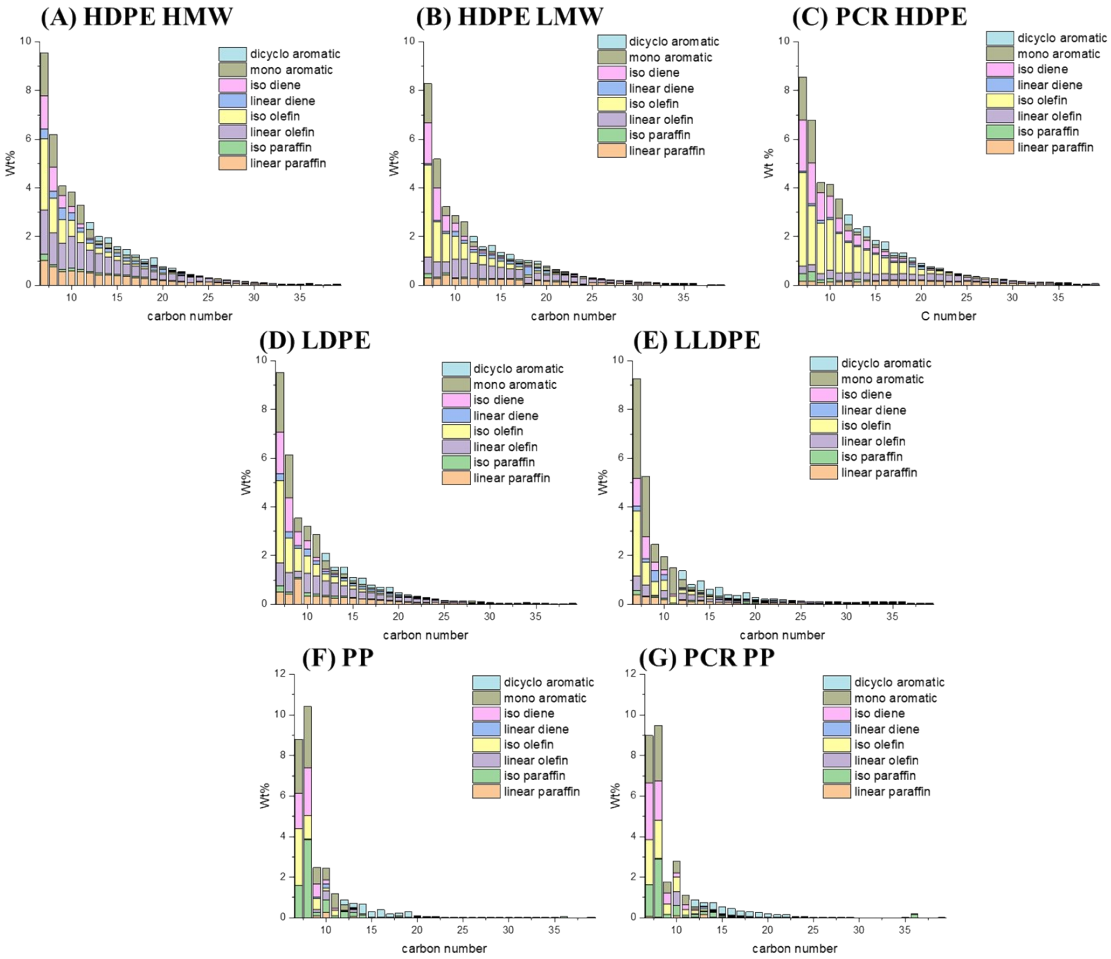

Fig. S8. The detailed product analysis from C7 to C40 with the branch analysis of (A) HDPE HMW, (B) HDPE LMW, (C) PCR HDPE, (D) LDPE, (E) LLDPE, (F) PP, and (G) PCR PP

5.6 Benchmark of Computational Methods

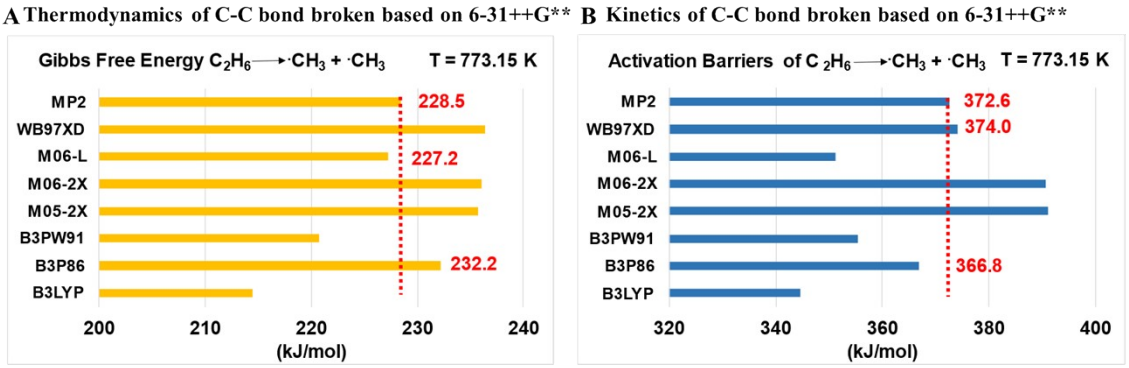

Fig. S9. Benchmark calculations for eight different DFT functionals for reaction Gibbs free energy and the activation energy barrier for C-C scission in C_2H_6 compared with the reference value calculated at MP2 level with the same basis set.

5.9 Model of LLDPE with different branch lengths

As displayed in Fig.S10, we calculated the barrier of the backbone and branch C-C scission in LLDPE with varying the branch length from methyl to ethyl, propyl, butyl, pentyl and hexyl as shown in dark blue and olivine filled circles and lines, respectively. Only methyl binding to C-C backbone can lead to a notably higher activation energy barrier for cleaving the branch (compared to cleaving the backbone). Increasing the length of the branch leads to a lower barrier for cleaving the branch but for ethyl and longer branches, the barrier no longer changes much. Hence, the branch's length has limited influence on the backbone C-C scission, with the most notable effect registered by going from methyl to ethyl. Therefore, the significant decrease of the barrier for the backbone C-C scission from HDPE to PP and LLDPE can be mostly attributed to the length of the branch (see details in the main text). Additionally, only methyl as branch (corresponding to PP) leads to the lower barrier of backbone broken than branch broken, which can explain the lower selectivity of PP pyrolysis towards methane, i.e., one of the major gas components. In contrast, the butyl as branch (corresponding to LLDPE) contributes to the lower energy cost of the C-C scission in branch than backbone, which leads to the highest selectivity towards gas.

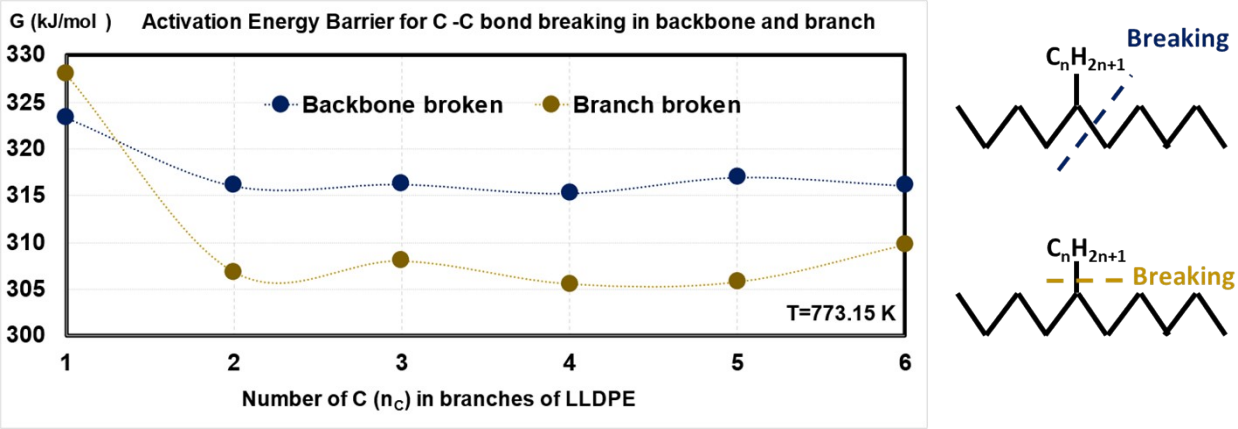

Fig. S10. The calculated activation energy barrier for C-C scission in backbone (dark blue filled circles and line) and branch (olivine filled circles and line) of LLDPE with the number of C in branch ranging from 1 to 6.

5.10. DFT predictions of HDPE and PP pyrolysis product distribution

To understand the origins of the inhibition effect that branches appear to have on gas production from PP observed in experiments (Table 1), we calculated the energy profiles (Fig.S11) for the most favorable pathways for the gasification of HDPE (red line) and PP (blue line). Both HDPE and PP start with backbone C-C scission, with activation energy barriers of 348.6 and 332.5 kJ/mol, respectively. The intermediate products pentane and 2-pentene from HDPE further decompose via subsequent backbone C-C scission and require an activation energy of 394.4 kJ/mol to produce gas products CH_4, C_2H_6, C_3H_6, and C_4H_6. In contrast, the subsequent backbone C-C scission in PP requires an activation energy barrier of 384.0 kJ/mol to yield gas CH_4, C_3H_6 together with liquid C_5H_8. Even though HDPE has a lower degradation barrier than PP, the full gasification of HDPE into gas components with carbon number below 5 leads to higher selectivity towards gas product than PP due to the unfavorable decomposition of methyl branch (Fig.S10). Hence, the presence of branches increases carbon number of pyrolysis products, which in turn triggers the incomplete gasification and favors liquid production. This is consistent with the much higher selectivity towards light oil from PP and LLDPE than HDPE observed in our experiments.

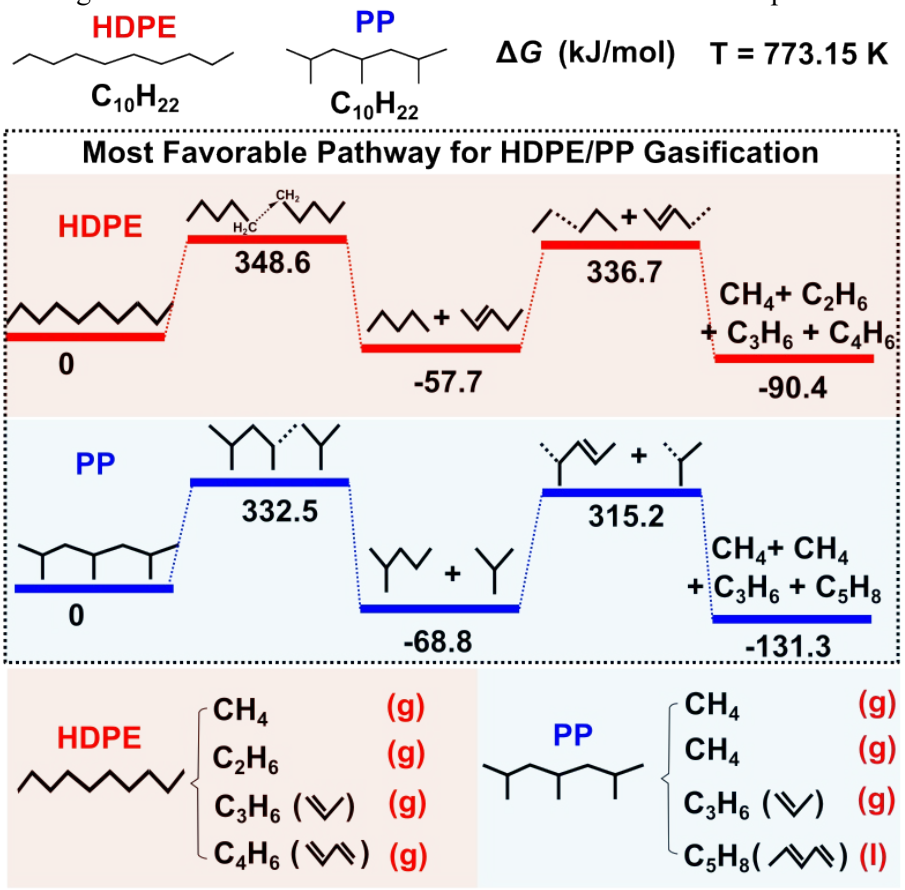

Fig. S11. The mechanisms for HDPE (red line) and PP pyrolysis (blue line) into gas components. (g) is used for gas; (l) is used for liquid.

References

1. Ditchfield, R.; Hehre, W. J.; Pople, J. A. J. T. J. o. C. P., Self-consistent molecular-orbital methods. IX. An extended Gaussian-type basis for molecular-orbital studies of organic molecules. **1971,** *54* (2), 724-728.
2. Petersson, a.; Bennett, A.; Tensfeldt, T. G.; Al-Laham, M. A.; Shirley, W. A.; Mantzaris, J. J. T. J. o. c. p., A complete basis set model chemistry. I. The total energies of closed-shell atoms and hydrides of the first-row elements. **1988,** *89* (4), 2193-2218.
3. Perdew, J. P. J. P. r. B., Density-functional approximation for the correlation energy of the inhomogeneous electron gas. **1986,** *33* (12), 8822.
4. Frisch, M. J.; Head-Gordon, M.; Pople, J. A. J. C. P. L., A direct MP2 gradient method. **1990,** *166* (3), 275-280.
5. Li, H.; Wu, J.; Jiang, Z.; Ma, J.; Zavala, V. M.; Landis, C. R.; Mavrikakis, M.; Huber, G. W., Hydroformylation of pyrolysis oils to aldehydes and alcohols from polyolefin waste. *Science* **2023,** *381* (6658), 660-666.
6. Yarkony, D. R. J. T. J. o. P. C., Current issues in nonadiabatic chemistry. **1996,** *100* (48), 18612-18628.
7. Harvey, J. N. J. J. o. t. A. C. S., DFT computation of the intrinsic barrier to CO geminate recombination with heme compounds. **2000,** *122* (49), 12401-12402.
8. Harvey, J. N. J. W. I. R. C. M. S., Spin-forbidden reactions: computational insight into mechanisms and kinetics. **2014,** *4* (1), 1-14.
9. McCaffrey, W. C.; Kamal, M. R.; Cooper, D. G., Thermolysis of polyethylene. *Polymer Degradation and Stability* **1995,** *47* (1), 133-139.
10. Altbach, M. I.; Fitzpatrick, C. P., Identification of conjugated diolefins in fossil fuel liquids by 1H n.m.r. two-dimensional correlated spectroscopy. *Fuel* **1994,** *73* (2), 223-228.
11. Offermann, W.; Mannschreck, A., Application of NMR spectroscopy of chiral association complexes. 14—chiral recognition of terpene and cyclohexene hydrocarbons by 1H and 13C NMR. *Organic Magnetic Resonance* **1984,** *22* (6), 355-363.